Investigating the effect of stairs on the bidirectional

movement of pedestrians

- \$" Rui Ye¹, Zhonghao Zhan¹, Mohcine Chraibi², Liping Lian^{3, 4}, Jun Zhang¹, Weiguo Song^{1*}
- % State Key Laboratory of Fire Science, University of Science and Technology of China, Hefei & 230027, People's Republic of China
- " Institute for Advanced Simulation, Forschungszentrum Jülich, Jülich 52425, Germany
- (" ³School of Urban Planning and Design, Peking University Shenzhen Graduate School, No. 2199,
-)" Lishui Road, Nanshan District, Shenzhen, 518055, China
- *" ⁴The Smart City Research Institute of China Electronic Technology Group Corporation, No.
- !+" 1006, Shennan Avenue, Futian District, Shenzhen, 518033, China
- !!" *Corresponding author: wgsong@ustc.edu.cn

!#" Abstract

! \$"

! %

! &" ! ' "

!("

!)"

| * "

#+"

#! "

##"

#\$"

#%

#' "

#("

#) "

#*"

\$+"

\$! "

\$#"

\$\$"

\$%

\$&"

\$' "

\$("

\$)"

\$*"

%"

%"

! "

#"

Although the bidirectional motion on stairs can be commonly observed for stairs outdoors and in some transportation facilities, a related study that aims to investigate pedestrians' walking characteristics under such condition has never been conducted. In this paper, we perform a controlled experiment to study the bidirectional stair motion with varying flow ratios. It is found that in average, the ascending pedestrians always walk slower than the descending ones independently on the flow ratio. At the same density, the average velocity is the smallest for the full bidirectional flow when compared with those in the descending and ascending ones, indicating that the full bidirectional flow is not a simple combination of unidirectional pedestrians from two directions. Besides, according to the individual time to collision, congestion level and crowd danger, the run when the flow ratio is 0.5 can be considered to be the most critical with a large number of fierce conflicts, thus the very balanced situation should be avoided intentionally for stairs where the bidirectional motion may occur.

#8" Keywords: stair motion, bidirectional flow, flow ratio, pedestrian dynamics

1. Introduction

As a special building structure that connects horizontal planes at different heights, stairs can be observed everywhere, from high-rise buildings to underground subway stations, and from indoor to outdoor. Due to the narrowed space and the existence of steps, stairs may act as a bottleneck during the movement of pedestrians, reducing their speed and even increasing the probability to fall. Crowd crushing and trampling accidents on stairs are frequently reported all over the world, especially in schools, stadiums, etc., leading to severe casualties. Indeed, pedestrian safety on stairs is a problem that should be studied and addressed urgently.

Since the 9/11 disaster, evacuation on stairs began to draw huge attention from researchers in different fields. Several large studies were conducted to collect basic evacuation data from survivors in that accident [1]. However, due to the fact that most of the derived data were obtained through questionnaires, interviews, etc., only results like delay time, evacuation time and global stair travel speed were roughly estimated [2, 3]. To get more detailed and accurate information about crowd movement on stairs, the evacuation drill has become a promising approach. Peacock et al. analyzed the video recordings of evacuation drills in eight office buildings and observed a wide range of local speeds (from 0.056 m/s to 1.7 m/s) within the same

! "

staircase [4]. Huo et al. conducted a stair evacuation in two scenarios, namely the phased evacuation and total evacuation, and emphasized the negative impacts of merging flow on the speeds of pedestrians from upstairs and egress efficiency in the total evacuation scenario [5]. What's more, Delin et al. confirmed and quantified the effect of fatigue during an ascending evacuation in long stairs [6]. In case of fire and power failure, evacuation by staircase may be affected as pedestrians become partly or even completely visually disabled. The influence of visibility (or illumination) was investigated by Chen et al. and Zeng et al. in [7, 8], and their experimental results indicated that generally, lower visibility reduced the walking speed and affected the position preference on stairs. Compared with normal adults, there exist special groups that need additional care and attention when egressing on stairs, such as children, the elderly and people with mobility impairments. Interestingly, children were found to move faster than adults on stairs in [9, 10]. In addition, according to [11, 12], the average walking speed on stairs for normal old adults was around 0.40 m/s, while for those with mobility impairments, the average speed was smaller than 0.30 m/s. In the meanwhile, models that can be used to simulate stair evacuation were proposed. Through grasping certain aspects of the movement of pedestrians on stairs, such as body rotation [13], the effect of step [14, 15] and the optimal velocity selection [16], simulation outputs may agree with the empirical data both at macroscopic and microscopic levels.

%#"

%\$"

%%' %&"

%"

%" %"

%"

&+" &! "

&#" &\$"

&%

&&"

&' "

&("

&) "

&* "

' +"

'!"

' #"

' \$"

' %"

' &"

1 1 11

' ("

')"

1 * 11

(+" (!"

(#"

(\$"

(%

(&"

('"

(("

()"

(*"

) +"

)!"

)#")\$"

)%"

)'"

The traditional manual counting method suffers from relatively large inaccuracies, resulting in discrepancy between different data from the literature. More recently, new progress in image processing and computer vision allowed to extract trajectory on stairs automatically, making it possible to analyze pedestrians' interactions more accurately [17, 18]. Based on precise trajectories, Burghardt et al. obtained a fundamental diagram for the descending flow, and they further presented vivid topographical profiles to indicate where high density and low velocity areas were located [19]. Chen et al. compared the fundamental diagrams from the descending and ascending flow via a single file motion, and found that the mean descending speed was larger than the ascending one from a statistical perspective [18]. Fu et al. focused on the characteristics of social groups on stairs and made comparison with those from the plane motion [20].

It should be noted that all the above-mentioned studies only focus on the unidirectional scenario. Concerning the bidirectional one, a stampede accident happened in the New Year's Eve of 2015 in Shanghai will be firstly mentioned. Due to the pushing of pedestrians that came from both directions (the descending and ascending direction), this accident led to 36 deaths and 49 injuries. It was not until then that we realized how deficient was our knowledge concerning this particular motion pattern. Actually, the bidirectional movement is a more common case for stairs outdoors and in some transportation facilities. Several related studies have been conducted so far. Cłapa et al. investigated the mutual interactions between the ascending firefighters and descending evacuees in a counter flow scenario, and decreasing speeds were observed in both movement directions [21]. Jiten et al. found that the function between flow ratio and capacity reduction displayed an asymmetric U shape for the bidirectional stair motion [22]. Chen et al. made a field study in two subway stations of Shanghai and obtained a fundamental diagram for the two-way stair traffic [23]. Besides, a model was built to simulate the uni- and bidirectional movement on stairs at different flow ratios in [24]. However, as far as the authors are concerned, a more in-depth study based on precise trajectories has never been conducted. Considering the fact that the bidirectional flow on stairs is often discontinuous and may be unbalanced, we designed and performed a controlled experiment at different flow ratios and with limited number of participants.

The remainder of the paper is organized as follows. In section 2 we introduce the experiment setup. In section 3 we present the detailed results. Finally, in section 4, we give our discussion and conclusion.

2. Experiment setup

The controlled experiment was performed on an outdoor staircase in the campus of University of Science and Technology of China in April, 2019. The staircase could be divided into two parts (upper and lower halves), connected by a mid-landing. To make the experiment setup as simple as possible, only the lower half of the staircase was chosen, which meant that we merely considered the movements of pedestrians on that part. A sketch of the experiment setup is shown in figure 1(b). The mock straight corridor was made up of six desks, with a width of 2 m to create relatively high density scenarios with limited participants. Totally there were 17 steps, with the step riser and step tread equal to 15 and 30 cm, respectively. Up to 100 Chinese university students were recruited to participate in our experiment, and their average age and height were 22.6 years old and 167.9 cm. The flow ratio r is defined as the number of descending pedestrians (N_d) , divided by the total number of participants (N_t) , namely $r=N_d/N_t$. Unlike the plane motion where flow ratio conditions like r and 1-r can be regarded as equivalent, for the bidirectional stair motion we set the flow ratio from 0.1 to 0.9 with a step of 0.1, due to the asymmetry between the descending and ascending flows.

Initially the participants were instructed to stand orderly in rows in the waiting areas on both sides according to the required numbers during that run. On hearing the starting command, they would walk across the mock straight corridor and leave it at the opposite side to avoid blocking other incoming pedestrians. To save time, runs with the opposite distributions of participants were conducted successively. For example, run r=0.1 was followed by run r=0.9 instead of run r=0.2, and the adjustment of participant numbers on two sides was done every two runs. In order to decrease effects due to fatigue, during the whole experiment, participants would have a short rest during their rearrangement in the waiting area after the completion of each run. For the convenience of experiment analysis, the whole movement process on stairs was recorded by two cameras that were fixed on the roof of that building.

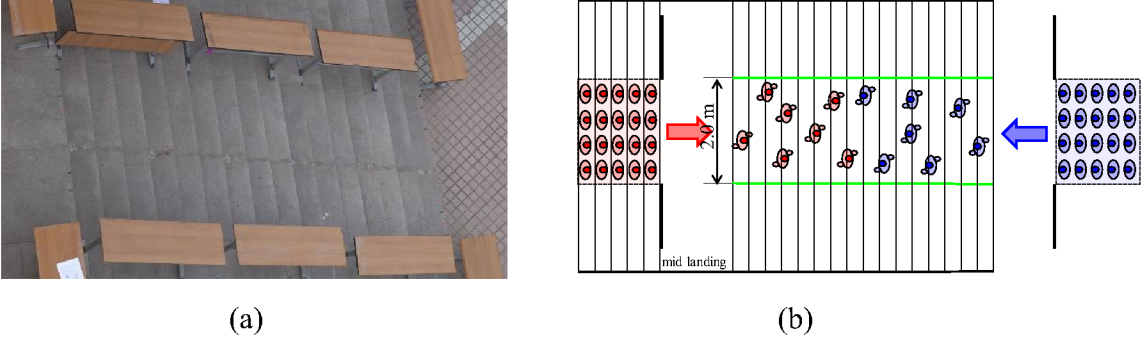


Figure 1. Illustration of the experiment setup. (a) Snapshot. (b) Sketch. In the sketch, the red ellipses donate those who move downstairs, and the blue ellipses are the ascending pedestrians.

Pedestrian trajectories are extracted through detecting colored hats with the *PeTrack* software automatically [17]. It should be noted that the colors of the hats are randomly distributed at the

very start of the experiment and do not provide information about pedestrians' walking directions. After obtaining the raw trajectories along the stair plane, they are further projected onto the horizontal plane, and all the results analyzed and discussed here will be based on the projected ones. Snapshot and corresponding trajectories for r=0.5 are presented in figure 2. Colors in the trajectories indicate the instantaneous x velocity. In all runs, usually two or three lanes are formed, due to the relatively narrow corridor and strong right walking preference. The two-lane condition happens when the bidirectional flow is rather unbalanced, and as it becomes more balanced, three-lane traffic will then appear. To investigate the lane formation process in our experiment, here we utilize the spatio-temporal diagram. The corridor is divided into uniform rows with a width of $0.2\,$ m. For each row, the relative number between descending and ascending pedestrians is calculated, namely $N_r(t)=N_d(t)-N_a(t)$. Then, we stack the relative numbers at same frame chronologically and obtain the diagram as shown in figure 2(c). Although in some runs (for example, r=0.5), some pedestrians may not choose to walk at their right side, but the number is relatively small, and the corresponding lane may soon vanish, at around $15\,$ s.

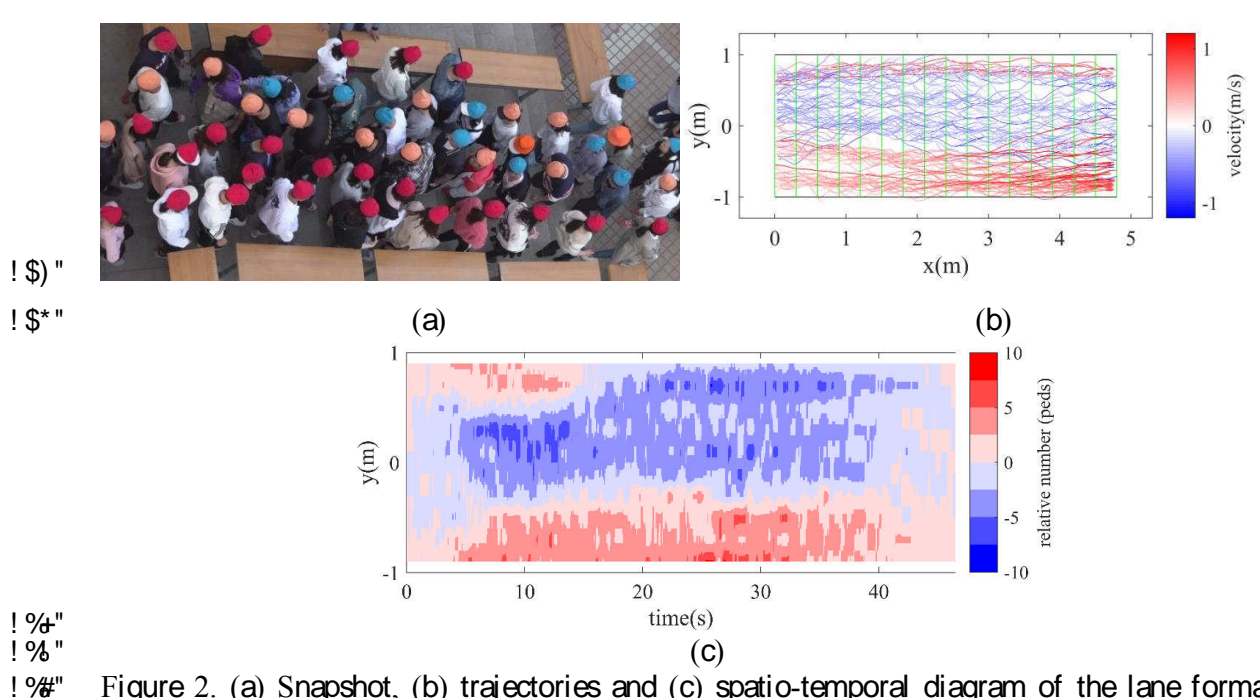


Figure 2. (a) Snapshot, (b) trajectories and (c) spatio-temporal diagram of the lane formation process when the flow ratio equals to 0.5.

3. Results and analysis

! #\$"

! #%

! #&"

!#"

!#(" !#)"

! #* "

! \$+"

! \$! "

! \$#"

! \$\$" ! \$%

! \$&"

! \$' "

! \$("

! %\$"

! %%

! %&"

!%"

! % "

! % "

! % "

! &+" ! &! " In this section, quantitative results about the crossing behaviors, fundamental diagram, time to collision (ttc) and congestion level will be analyzed and discussed.

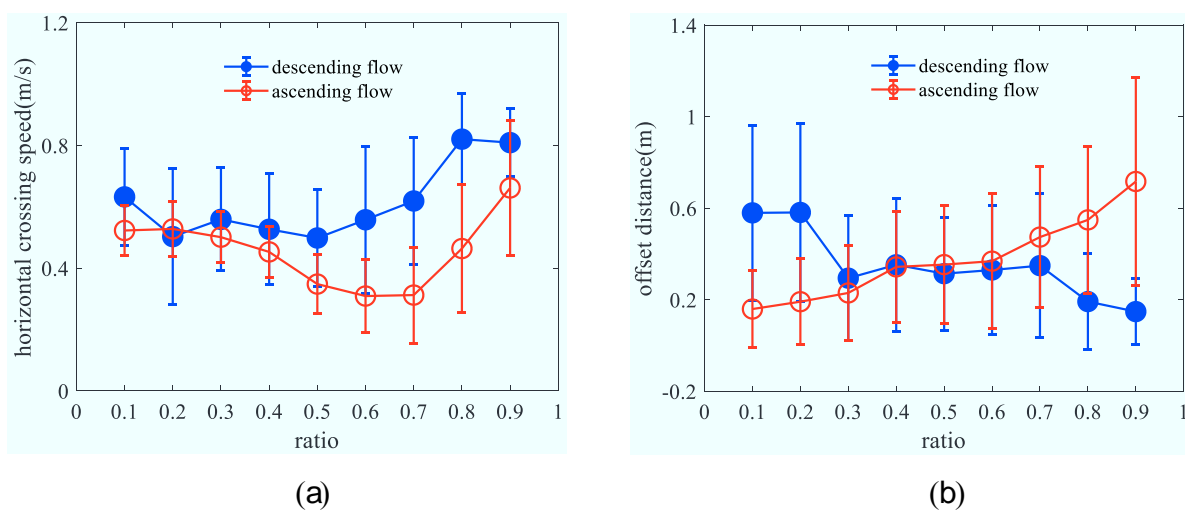
3.1 Crossing behaviors

We define two quantities to describe the crossing behaviors of pedestrians, separately the horizontal crossing speed and the offset distance. The horizontal crossing speed is defined as the horizontal length of the stairs (L, which is $4.8\,$ m for all pedestrians), divided by the crossing time ($t_{crossing}$), namely $v_{crossing}$ =L/ $t_{crossing}$. Meanwhile, the offset distance is defined as the relative lateral

displacement between the entering and exiting positions of the mock straight corridor, namely $d_{\text{offset}} = \left| y_{\text{exit}} - y_{\text{enter}} \right|$, which can reflect the collision avoidance behavior of pedestrians to some extent. Corresponding statistical results are displayed in figure 3.

From figure 3(a), it can be found that apart from the run when the flow ratio equals to 0.2, the average crossing speeds for the descending pedestrians are always larger than those for the ascending ones, in contrast with the result shown in [25] for plane motion, according to which a significant difference of crossing speeds between pedestrians from two directions only occurs for r<0.3. For this, the reason is not hard to explain. During the ascending process, pedestrians have to overcome the gravity, thus resulting in longer crossing time and smaller crossing speeds. Indeed, the existence of gravity is rather influential for the movement on stairs. Besides, for pedestrian flows from both directions, with the increase of flow ratio, the average crossing speed will firstly decrease and then increase, but interestingly, the minimum crossing speeds are located at two different flow ratios. For the descending flow, the minimum is found at r=0.5, while for the ascending flow it is found at r=0.7.

As indicated by the average values of offset distance in figure 3(b), pedestrians will make lateral movement to avoid collisions with others in all runs. No matter for the descending or ascending flow, the largest average offset distance (up to around 0.6 m) occurs in the minor flow under the unbalanced bidirectional condition, namely r=0.1, 0.2, 0.8 and 0.9. In these four runs, there are only 10 or 20 pedestrians in the minor flow, thus they can move in a more flexible manner and tend to be more active to make detour path to avoid incoming pedestrians, which is also the reason why the average crossing speed begins to increase for r>0.7 in the ascending flow. In the meanwhile, the values of offset distance are low in the corresponding major flow in these four runs. As for other runs, this value stays relatively stable and no much difference can be found between two movement directions.



!()" Figure 3. Statistical results about the crossing behaviors of pedestrians. (a) Horizontal crossing !(*" speed. (b) Offset distance.

!)+" 3.2 Fundamental diagram

! &#"

! &\$" ! &%"

! &&" ! &' "

! &(" ! &) "

! &* "

!'+" !'!"

!'#" !'\$"

!'%" !'&"

!''"

!'("

!')"

!'*"

! (+"

!(!" !(#"

! (\$"

! (%

! (&"

!('"

!(("

!)!"

!)#" !)\$" Since our experiment is conducted at relatively high global densities, to obtain a wide density range, here we adopt the method based on the Voronoi diagram to explore the microscopic fundamental diagrams [26]. In this method, each pedestrian i at time t will be assigned an

individual density $(\rho_i(t))$ according to the area of the Voronoi cell that belongs to him/her $(A_i(t))$, namely

186
$$\rho_i(t) = 1/A_i(t)$$
. (1)

The velocity magnitude of pedestrian i at time t can be calculated as follows:

189

190

191

192193

194

195

196 197

198

199

200

201

202

203

204

205206

207

208

209

210

211

212

213

214215

216

217

218

188
$$v_i(t) = \left\| \frac{\vec{x}_i(t + \Delta t/2) - \vec{x}_i(t - \Delta t/2)}{\Delta t} \right\|,$$
 (2)

where $\vec{x}_i(t)$ represents the position of pedestrian *i* at time *t* and Δt is a time interval equal to 0.4 s. After obtaining the density and velocity, the specific flow is calculated as the product of them.

To compare the fundamental diagrams, here we focus on three states within the whole corridor, that is, the full bidirectional flow (where bidirectional movement covers the whole space of the corridor), pure ascending flow (where only ascending pedestrians cover the whole corridor) and pure descending flow (similar to pure ascending flow), which means that data during other states like lane formation and lane dissolution (for a more detailed classification of flow states in the bidirectional scenario, please refer to [25, 27]) are excluded and not considered in our study. After manually recognizing these three states through the video recording of each run, data are extracted. To make it more clear, the exact runs from which data in a certain state are derived are listed in table 1. The raw data are plotted in figure 4(a).

Table 1. Illustration about the data extraction of fundamental diagrams.

State	Flow ratios
Full bidirectional flow	0.2, 0.3, 0.4, 0.5, 0.6, 0.7, 0.8
Ascending flow	0.1, 0.2, 0.3, 0.4
Descending flow	0.8, 0.9

From the scatter plot, we obtain fundamental diagrams that cover a wide density range, especially for the full bidirectional flow. In the unidirectional scenarios, it is observed that for the ascending flow, the velocity at the same density is smaller than that for the descending flow, and higher density can be reached during the ascending process, although the inflow rate may be almost identical. This indicates that the bottleneck effect of the ascending movement is more obvious than the descending movement. Besides, in the full bidirectional flow, high individual density up to 7 ped/m² appears, and the values of the specific flow range from almost 0 to 4 ped/(m·s), which is quite dispersed. To quantify such dispersion, the fan chart plot where velocities within each density interval (0.1 ped/m²) are displayed at different percentiles (from the 5th percentile to the 95th percentile with a step of 5 percentiles) is given in figure 4(b). In this plot, the specific flow increases with the density for all states. Besides, for the velocity data within one certain density interval, the full bidirectional state has the widest distribution, indicating that it's the most complex movement pattern among these three states, and in the meanwhile the descending flow is the simplest one with least uncertainty. Also, the fundamental diagram for the bidirectional flow does not lie between those for the descending and ascending flow, meaning that the bidirectional stair movement is not a simple mixture of pedestrians from two directions, and their interactions also matter a lot during the entire movement process. Actually, when a bidirectional movement occurs on stairs, the traffic capacity will decrease.

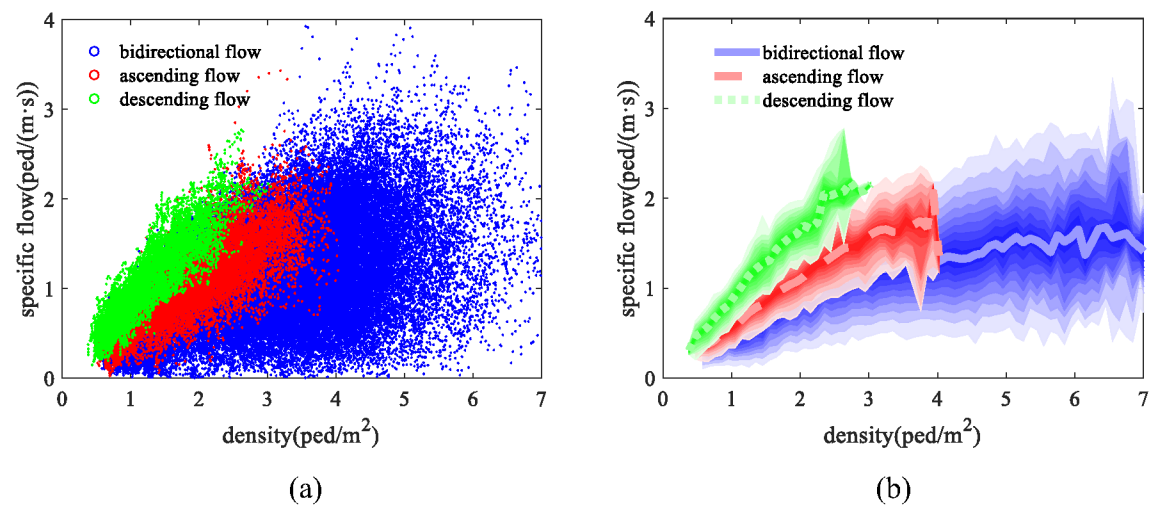


Figure 4. Fundamental diagrams for three movement states on stairs. (a) Scatter plot. (b) Fan chart plot.

Next we further compare the fundamental diagrams at different flow ratios. For all runs, the binned data can be fitted using quadratic functions in the following form: $J_s=k_1\rho+k_2\rho^2$, with high values of \mathbb{R}^2 . Compared with the fundamental diagram in the balanced run, higher values of specific flow can be found in the unbalanced runs especially for densities above 3 ped/m² (see figure 5(a)). In the unbalanced runs, either the descending flow or ascending flow will play the dominant role as there are too few pedestrians in the opposite direction. Under this condition, the bidirectional stream behaves more like a unidirectional one, although the plotted data are truly extracted from the full bidirectional state of that run. What's more, if the descending flow is the domiant one (r=0.8), the capacity will be even higher than that when r=0.2. On the other hand for the more balanced runs, as shown in figure 5(b), difference is not that significant (although it still exists) because the numbers of pedestrians from two sides become more comparable within the whole corridor.

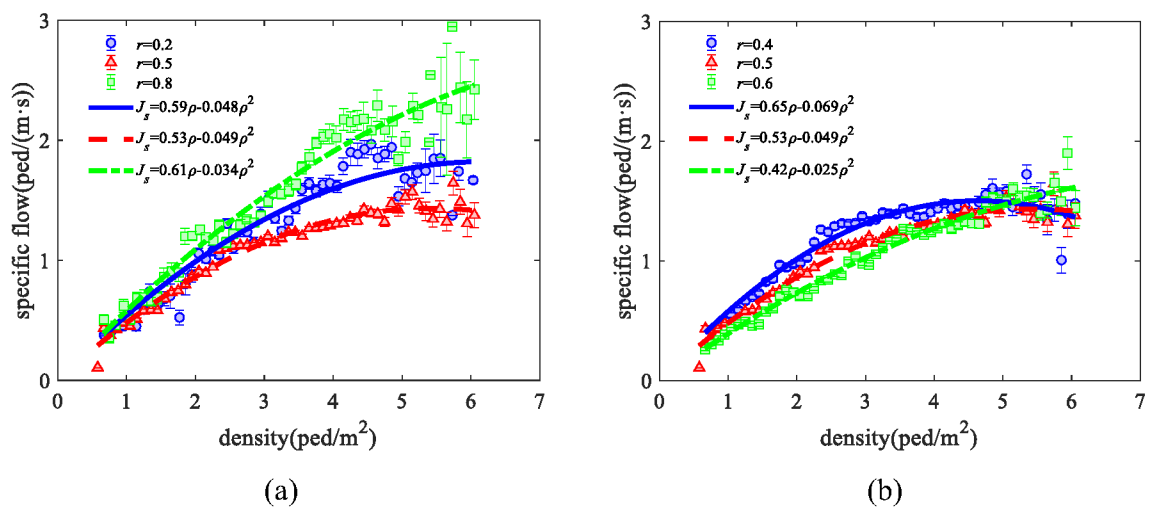


Figure 5. Comparisons of the fundamental diagrams at different flow ratios. (a) r=0.2, 0.5 and 0.8. (b) r=0.4, 0.5 and 0.6.

3.3 Time to collision

The concept of time to collision (*ttc*), introduced by Karamouzas in [28] to model pedestrian dynamics, is known to be useful to realize the collision avoidance between two interacting pedestrians in simulation models. Inspired by the work of Holl where the relations between time to collision and density are obtained for the multidirectional flows [29], we also hope to utilize this new concept in our own experiment to quantify the degrees of collisions for the bidirectional stair streams at varying flow ratios.

For the sake of completeness, we introduce the calculation method of time to collision briefly. Assuming that pedestrians i and j are two persons that are randomly selected from the crowd within the corridor, let us denote their positions and velocities by \vec{x}_i , \vec{x}_j and \vec{v}_i , \vec{v}_j , as shown in the sketch of figure 6. To get t_1 and t_2 , the following equation should be solved:

250
$$\|\vec{x}_i + \vec{v}_i \cdot t - (\vec{x}_j + \vec{v}_j \cdot t)\| = d_{ij},$$
 (3)

- where d_{ij} is the distance between these two pedestrians when they just touch each other, which
- equals to 0.4 m as each pedestrian is usually simplified as a circle with the radius of 0.2 m.
- Furthermore, the above equation can be reorganized into the following form:

$$254 at^2 + bt + c = 0, (4)$$

- where $a = (\vec{v}_i \vec{v}_j)^2$, $b = 2(\vec{x}_i \vec{x}_j)(\vec{v}_i \vec{v}_j)$ and $c = (\vec{x}_i \vec{x}_j)^2 d_{ij}^2$. Then we only need to
- consider the situation when $\Delta = b^2 4ac > 0$. Supposing that $t_1 < t_2$, there are three conditions:
- 257 (1) If $t_1 < 0 \& t_2 < 0$, ttc_{ij} does not exist.
- 258 (2) If $t_1 < 0 < t_2$, $ttc_{ij} = 0$.
- 259 (3) If $t_1 > 0 \& t_2 > 0$, $ttc_{ii} = t_1$.

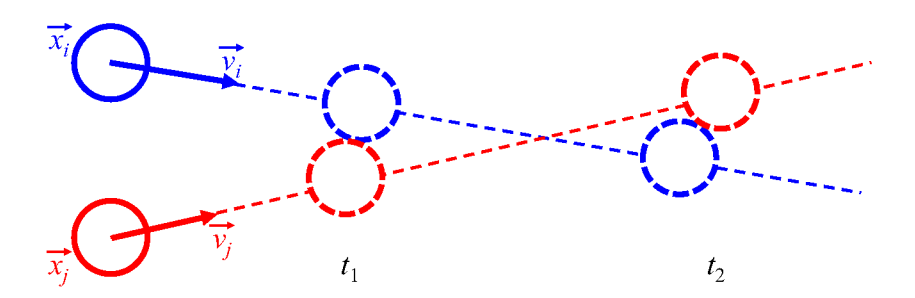
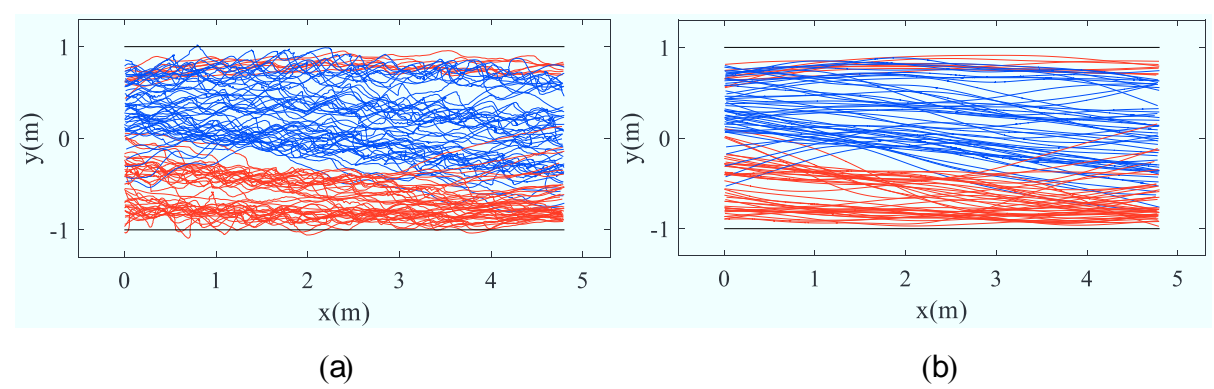


Figure 6. Sketch of the calculation of time to collision. Here t_1 and t_2 are the roots of equation (4) and denote the time of initial and final overlapping.

Before calculating the time to collision, another important issue that should be addressed beforehand is that the trajectories extracted based on the head movements usually sway, therefore the actual movement direction cannot be obtained directly from the raw data. Thus a preprocessing step to smooth them is necessary. For this purpose, we use a MATLAB function named csaps based on the cubic smoothing splines to eliminate the sways in trajectories from all runs. A comparison before and after smoothing when r=0.5 can be found in figure 7, which clearly proves that the smoothing method that we choose is effective.



#(+" #(!"

#(#"

#(\$"

#(%

#(&"

#('"

#(("

#()"

#(*"

#) +"

#)#"

#) \$"

#)%

#) &" #) ' "

#)(" #))"

#) * "

#* +"

#*!"

#*#"

#*\$"

#*%

#* &"

Figure 7. Comparison of trajectories before and after smoothing when the flow ratio is 0.5.

For a certain pedestrian i at time t, his/her time to collision $ttc_{i,t}$ should be the smallest positive root from equation (4) between him/her and any other pedestrian j in the corridor. Since pedestrians are mainly reacting to collisions happening in the close future, behaviors corresponding to high values of ttc are basically equivalent. Nevertheless, ttc can assume arbitrarily high values, and such values may strongly influence the average value of ttc. For this reason, in the following we will restrict its value to a reasonable threshold, t=10 s. Firstly we focus on the time series of average ttc, which can be calculated as follows with N indicating the total number of pedestrians at time t:

#)!"
$$ttc_{t} = \frac{1}{N} \sum_{i=1}^{N} ttc_{i,t}$$
. (5)

The time series data of average ttc at six flow ratios are given in figure 8. During the first few seconds, the average ttc will decrease, and such decrease gets more intense especially in the unbalanced runs. Then it will keep relatively stable, apart from r=0.3. The more balanced the bidirectional flow is, the longer duration of the steady state becomes. The dashed blue lines in the plots indicate the end of the full bidirectional flow, which are extracted manually through observing the video recording. The time when the average ttc begins to increase is almost consistent with the position of the dashed blue line, which is not hard to explain. After the full bidirectional state, lanes begin to dissolve. Density in the corridor will decrease and fierce conflicts happen less frequently, which makes the average ttc increase. Besides, after the increase process, there will appear another steady state in some runs. The fact is that during this state, the bidirectional flow has transferred into a unidirectional one either along the descending or ascending direction because pedestrians from one direction have been all cleared. In addition, the average values of ttc during this new state depend on the movement direction of the unidirectional flow.

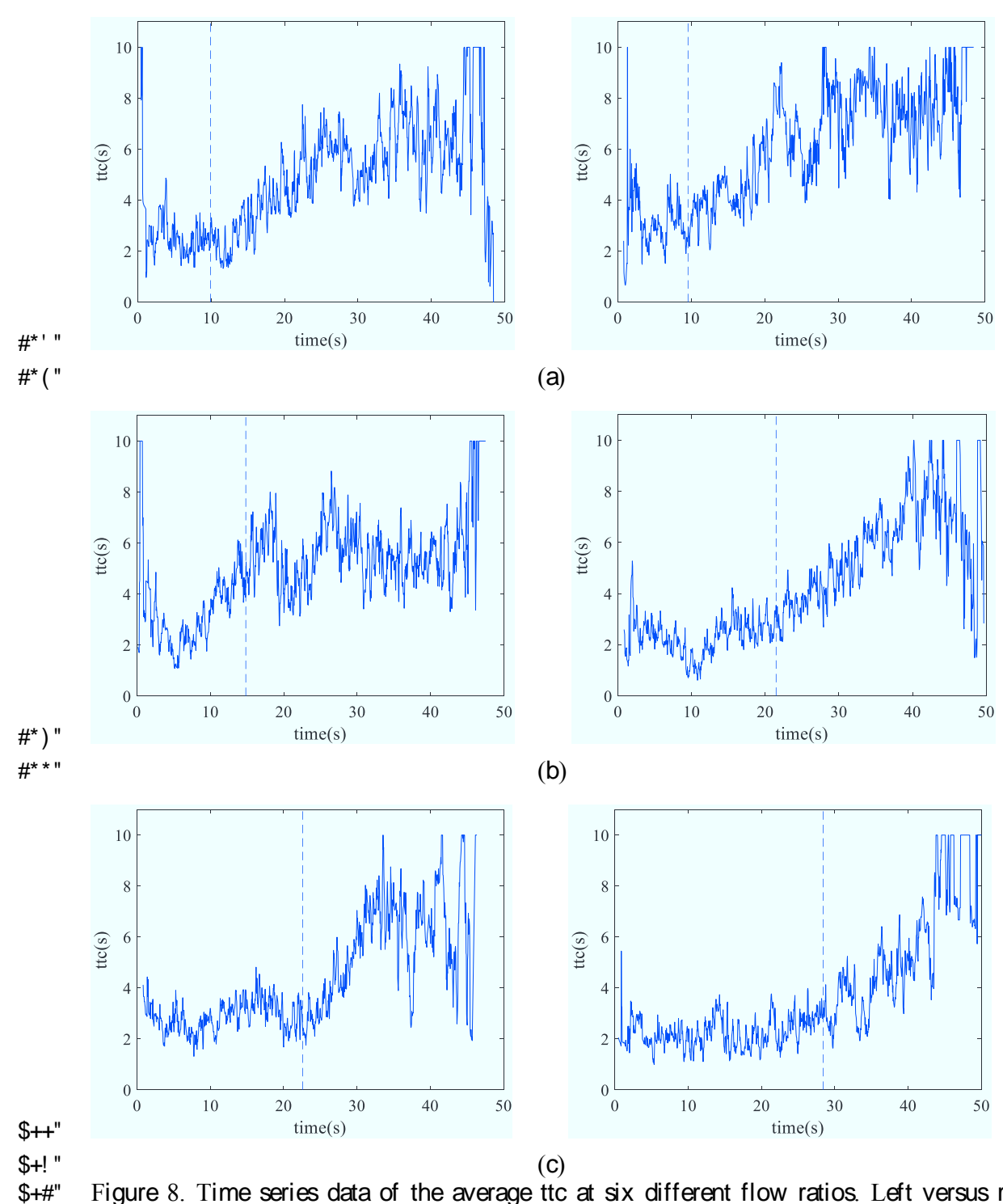


Figure 8. Time series data of the average tic at six different flow ratios. Left versus right: r versus (1-r). (a) 0.2 versus 0.8. (b) 0.3 versus 0.7. (c) 0.4 versus 0.6.

\$+\$"

\$+%

\$+&" \$+' "

\$+("

The values of individual ttc for all runs are presented in a box plot as shown in figure 9(a). The relations of both median and average values with the flow ratios exhibit an asymmetric U shape, which is also caused by the difference in movement pattern between the descending and ascending pedestrians. It can also be found that the most intense conflicts happen when r equals

to 0.5 and 0.6, with the median values approximating to 1 s. Also, in these two runs, many values of the individual ttc are 0 s, meaning that many pedestrians will touch or overlap with others around in the crowded corridor, based on our approximation of pedestrians as R=0.2 m circles in equation (4). Besides, data about different flow states are displayed in figure 9(b), and the values in the full bidirectional flow are far smaller than those in the unidirectional flow, due to higher global density and more chaotic velocity direction. In addition, the difference of values between the descending and ascending flow can be explained by the cue found in the fundamental diagrams as shown in figure 4. At the same density, the velocity variance in the descending process is smaller than that in the ascending one, resulting in a situation where pedestrians are moving in a more ordered and uniform manner, with very similar velocities. Consequently, fewer collisions, or milder collisions will happen when they are descending.

\$+)"

\$+*"

\$! +"

\$!!" \$!#"

\$! \$"

\$! %' \$! &"

\$! ' "

\$! ("

\$!)"

\$! *"

\$#+"

\$#! "

\$##" \$#\$"

\$#%

\$#&"

\$#' " \$#("

\$#)"

\$#*"

\$\$+" \$\$! "

\$\$#"

\$\$\$"

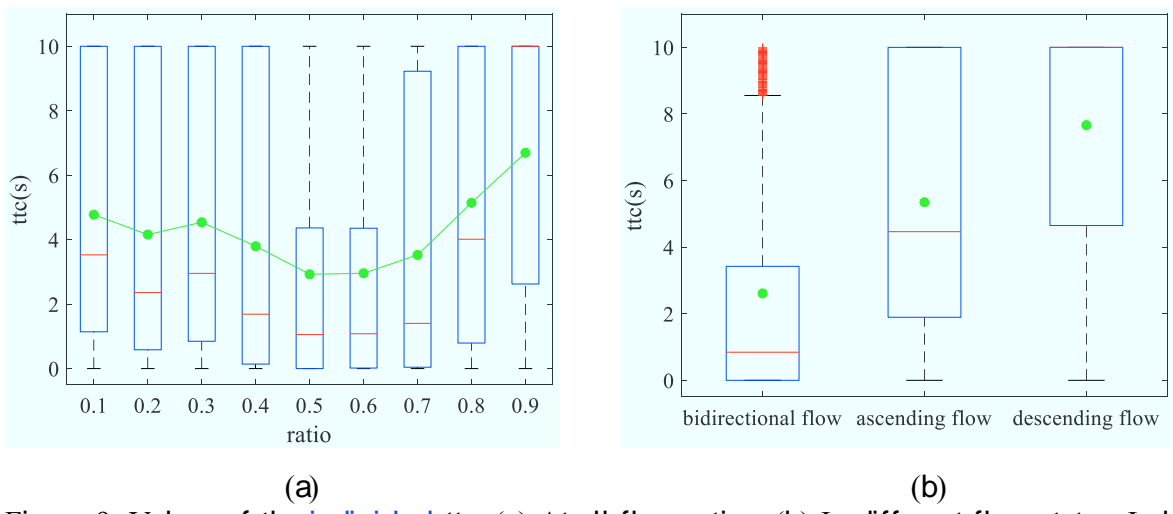
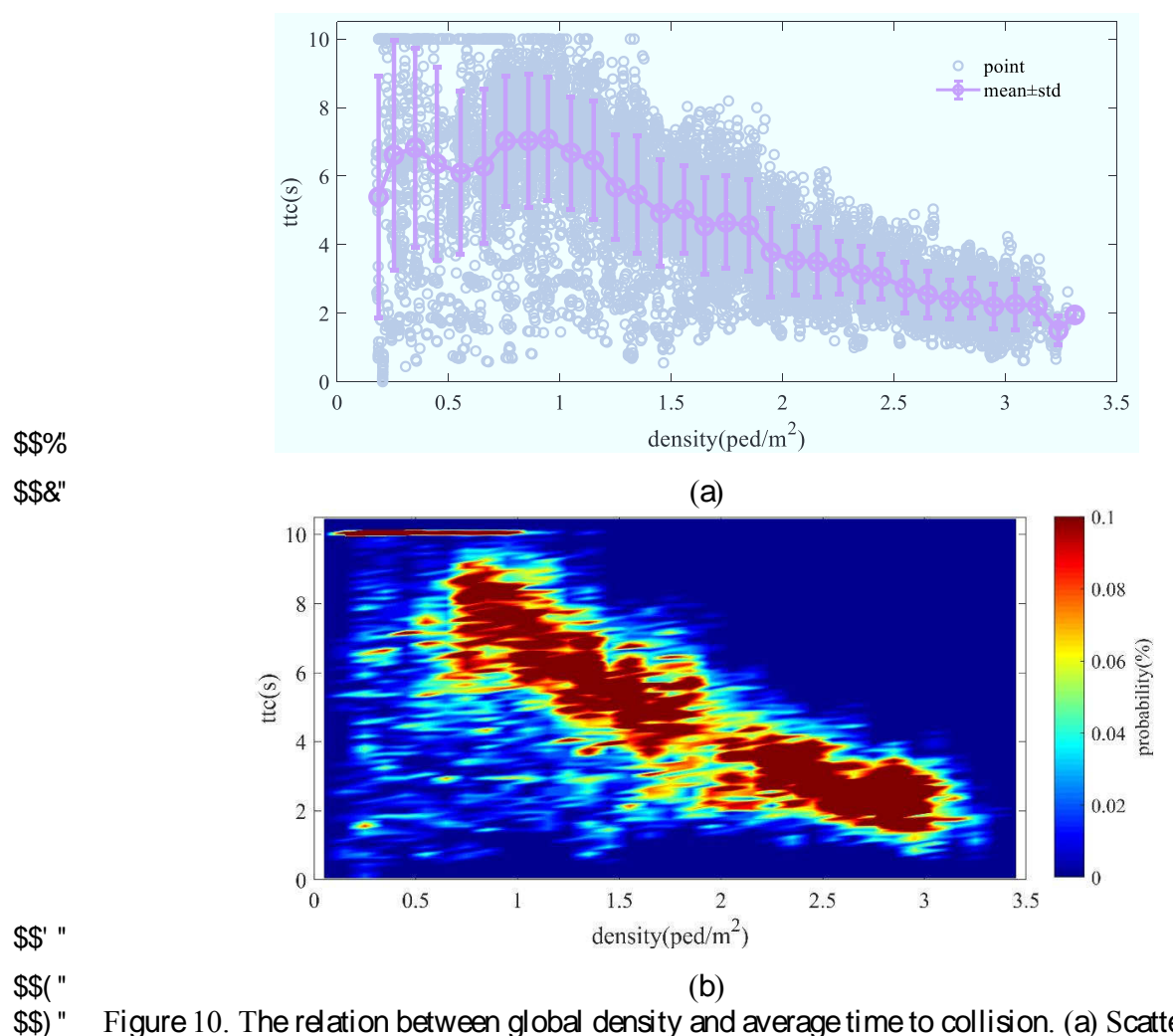


Figure 9. Values of the individual ttc. (a) At all flow ratios. (b) In different flow states. In both plots shown above, the horizontal solid red lines and solid green dots represent the median and average values, respectively. The red '+' symbols represent the outliers.

We also explore the relation between density and average ttc. The density here is calculated as the global one within the whole corridor based on the Voronoi diagram [26], thus the highest value is just about $3.4~{\rm ped/m^2}$. To get the relation, data from all nine runs are combined. Although the grey data points in figure 10(a) exhibit dispersion, from the mean values and the distribution shown in the heat map, it can be clearly seen that the average time to collision decreases with the increase of density for $\rho > 0.75~{\rm ped/m^2}$. With the corridor becoming even crowded, pedestrians will collide with another one more easily, which is reflected in the decrease of ttc. Besides, we also notice that when the density is low, there are still some data points with small values of ttc. This mainly happens when pedestrians just enter the stair corridor, and make detours to avoid collisions with the opposite flow.



\$\$*"

\$%+"

\$%"

\$%#"

\$%\$" \$%%

\$%&" \$% "

\$%"

\$%)"

\$%"

\$&+"

\$&! "

\$&#"

\$&\$"

\$&%" \$&&"

Figure 10. The relation between global density and average time to collision. (a) Scatter plot with the purple circles and error bars representing the mean values and standard deviations using a bin size of 0.1 ped/m^2 . (b) Distribution of the data points in the relation with a grid size of $0.1 \, ! \, 0.1$.

As mentioned earlier, ttc is defined as the time when pedestrian i has the first collision with a certain pedestrian j, if they keep on moving with current velocity. To have a more in-depth understanding of the mutual interactions among pedestrians, we further calculate their relative positions, or to be more precise, the position of pedestrian j relative to pedestrian i. Since large values of ttc (here above $10\,$ s) can be neglected, the corresponding relative positions are not visualized in the results of 4 runs presented in figure $11.\,$ Notably, in the left panel of the figure, the magenta circle at the origin represents the current pedestrian i, and his/her velocity direction is pointing towards the right, namely the direction of the positive x axis.

Generally, we can say that the closer these two pedestrians are, the smaller the value of ttc will be. Meanwhile, one can also observe small values of ttc (larger than 1 s) located at far distances up to 4 m, which is caused by the head-on conflicts between pedestrians from two directions when they just enter the corridor. As a result, the relative positions for each run display a front-back asymmetry, with it being more pronounced in the balanced runs, since the head-on conflicts are fiercer in these runs during the initial stage. Around the magenta circle, a hollow ring does not exist, which implies that the overlapping is a common case in our experiment even at

moderate density. In addition, although the distribution for every run covers a wide range, the positions with relatively large probability are mainly within an ellipse, as indicated by the grids that are not marked in blue in the right panel of the figure. Also, the size of this ellipse is smaller in the balanced run than that in the unbalanced run, due to different global densities in different runs.

\$&' "

\$&("

\$&)"

\$&*"

\$' +"

\$(+" \$(!"

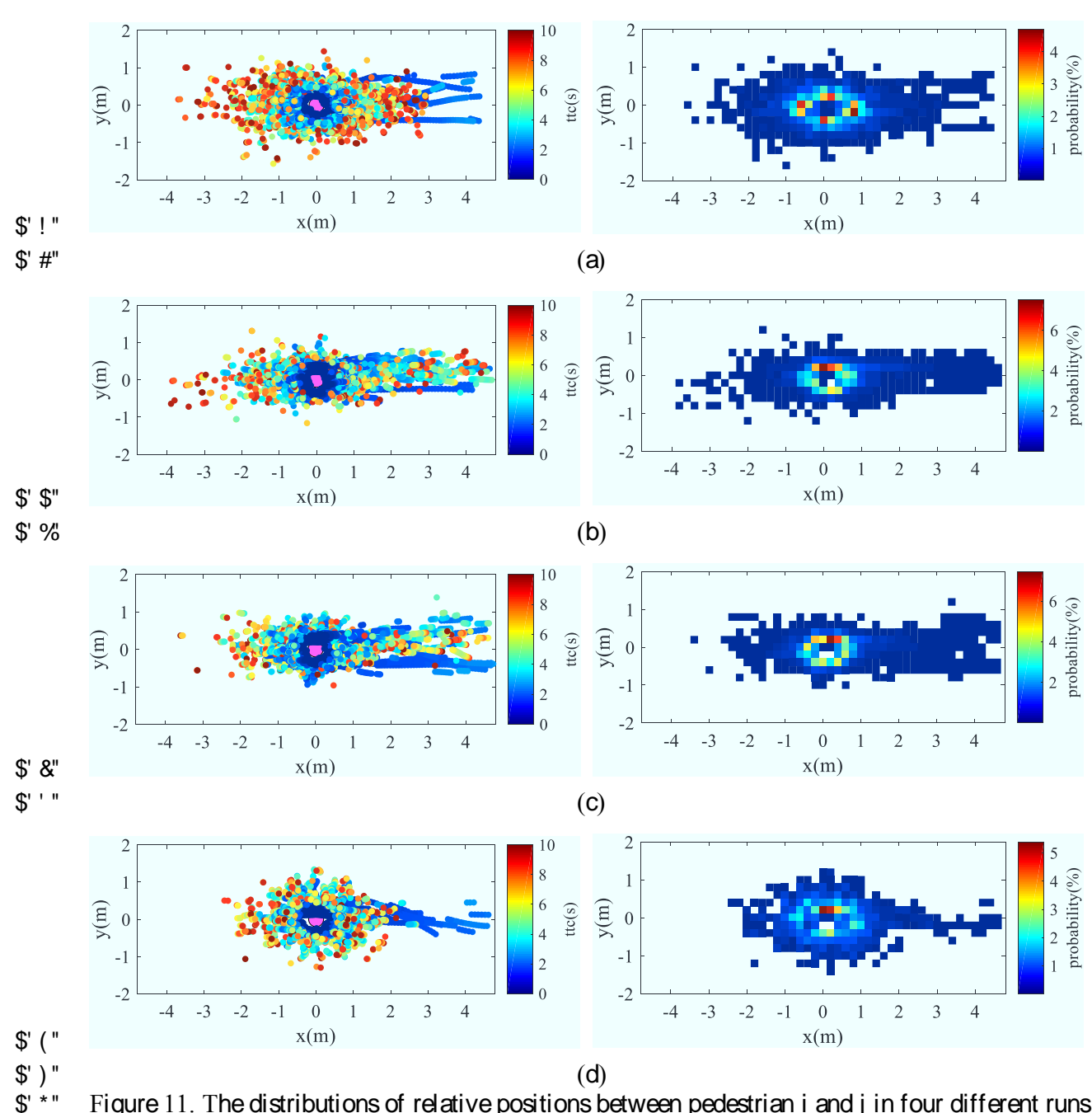


Figure 11. The distributions of relative positions between pedestrian i and j in four different runs (left panel: scatter plot, right panel: heat map with a grid size of $0.2 \,!\: 0.2 \, \text{m}^2$). (a) r=0.1. (b) r=0.5. (c) r=0.6. (d) r=0.9.

We further divide i, j as pairs in the same or contrasting flow, and the results for r=0.1 and 0.5 are shown below in figure 12. For other flow ratios, similar outcomes can be obtained. The results are a little surprising to us because the number of first collisions which happen in the contrasting flow is far smaller than that in the same flow, and most of them are located in front. But it's actually reasonable as very stable lane formation can be observed in our experiment, which means that pedestrians mainly interact with others in the same lane during this period. This also provides new insights into the modelling of lane formation in bidirectional scenarios. For the left panel, the distributions are more symmetrical after filtering out those points from the contrasting flow.

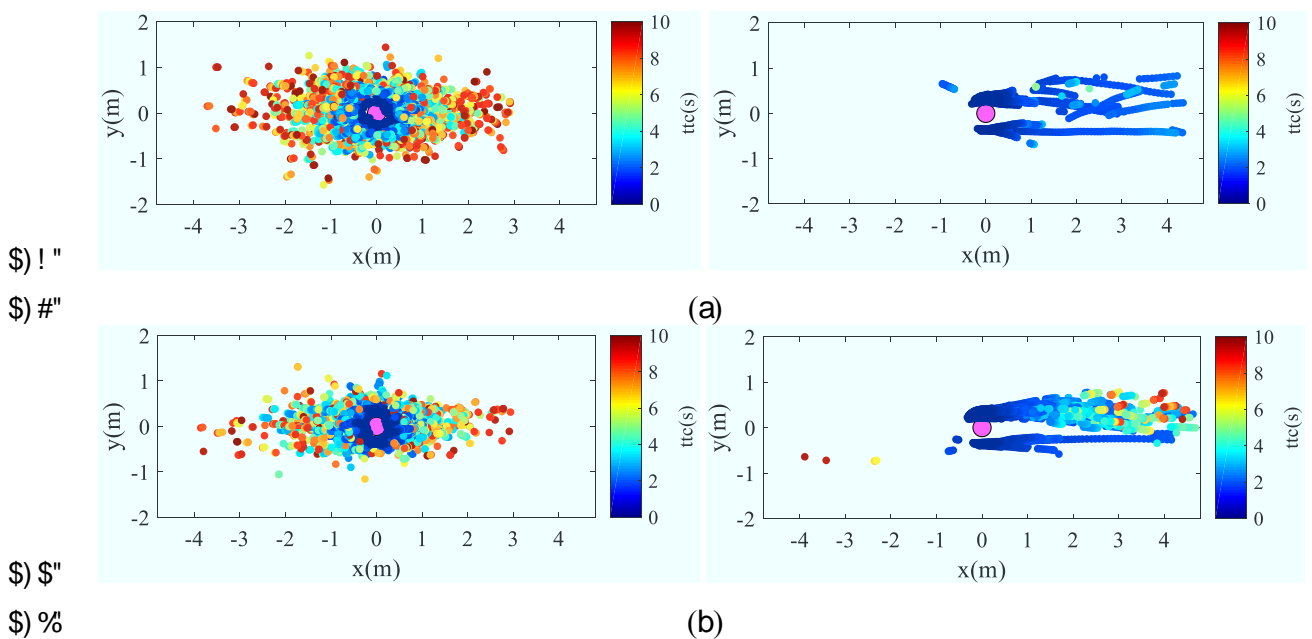


Figure 12. The distributions of relative positions between pedestrian i and j when they are divided based on whether in the same or contrasting flow (left panel: same flow, right panel: contrasting flow). (a) r=0.1. (b) r=0.5.

3.4 Congestion level

\$(#"

\$(\$"

\$(%

\$(&"

\$('"

\$(("

\$()"

\$(*"

\$) +"

\$) &"

\$)'"

\$)("

\$))"

\$) * "

\$*+"

\$*!"

\$*#"

\$*\$"

\$*%

\$* &"

\$*'"

\$*("

\$*)"

To make a quantitative measurement about the congestion and intrinsic risk in the bidirectional crowd at varying flow ratios, the recent concepts of congestion level and crowd danger draw our attention [30]. Compared with the crowd pressure that is proposed in [31] for the analysis of a crowd disaster happened during the Hajj at extremely high density, the congestion level and crowd danger are more suitable to estimate the crowdedness and intrinsic risk in controlled experiments at comparatively lower density.

There are altogether three steps to compute the congestion level. First of all, the whole corridor space is divided into square grids with the size of $0.2 \,!\, 0.2 \, \text{m}^2$. For any grid (i, j), an average velocity vector is calculated based on the trajectory information during a time interval of 3 s. Then, the rotation of the velocity vector field can be obtained:

399
$$\vec{R}(x,y) = \begin{pmatrix} r_x \\ r_y \\ r_z \end{pmatrix} = \nabla \times \vec{v}(x,y).$$
 (6)

Finally, the congestion level is calculated using the following equation:

410

411 412

413

414

415 416

417

418

419

420

421

422

423

424

425

426

$$401 Cl = \frac{\max(r_z) - \min(r_z)}{|\vec{v}|}, (7)$$

where $\max(r_z) - \min(r_z)$ denotes the rotation range for grids over the Region of Interest (ROI). It should be noted that for a 2d velocity vector field, only r_z will have non-zero values. Besides, $|\vec{v}|$ is the average value of the velocity vector field obtained in step one within the ROI (those grids with null values are excluded). For simplicity, here we consider the whole area of the corridor as the ROI, and calculate the rotation range and congestion level at a global level. We further compute the global crowd danger, by multiplying the global congestion level and density with the following equation:

$$409 Cd = Cl \cdot \rho. (8)$$

For each run, to obtain the values of rotation range, congestion level and crowd danger at continuous frames, we move the time interval from the starting frame to the ending frame with a step of 1 frame. Typical results in three runs are displayed in figure 13. Usually, the congestion level is high during the initial stage of each run, which is due to pedestrians' collision avoidance behaviors. Besides, we also observe that the values at varying flow ratios show distinguished difference especially for those in the most balanced and unbalanced runs. Indeed, compared with the unbalanced runs, there are more fierce conflicts and avoidances within the whole duration in the balanced runs. Especially, for r=0.1, the corresponding values are mostly larger than those in r=0.9. For these two runs, after 10 descending or ascending pedestrians have all left the corridor, there will be a pure ascending or descending process. Although the boundary condition, namely the entrance and exit width is same, the density in the corridor is higher in the ascending process due to slower walking speeds of ascending pedestrians. Besides, as indicated by the fundamental diagrams in figure 4, speeds in the ascending process are more heterogeneous, which makes collisions happen more easily, resulting in smaller individual ttc as shown in figure 9(b). Thus, values for the congestion level are higher in r=0.1 than r=0.9. Furthermore, compared with the congestion level, the difference in crowd danger for these three runs is even more significant because density in the corridor is also considered.

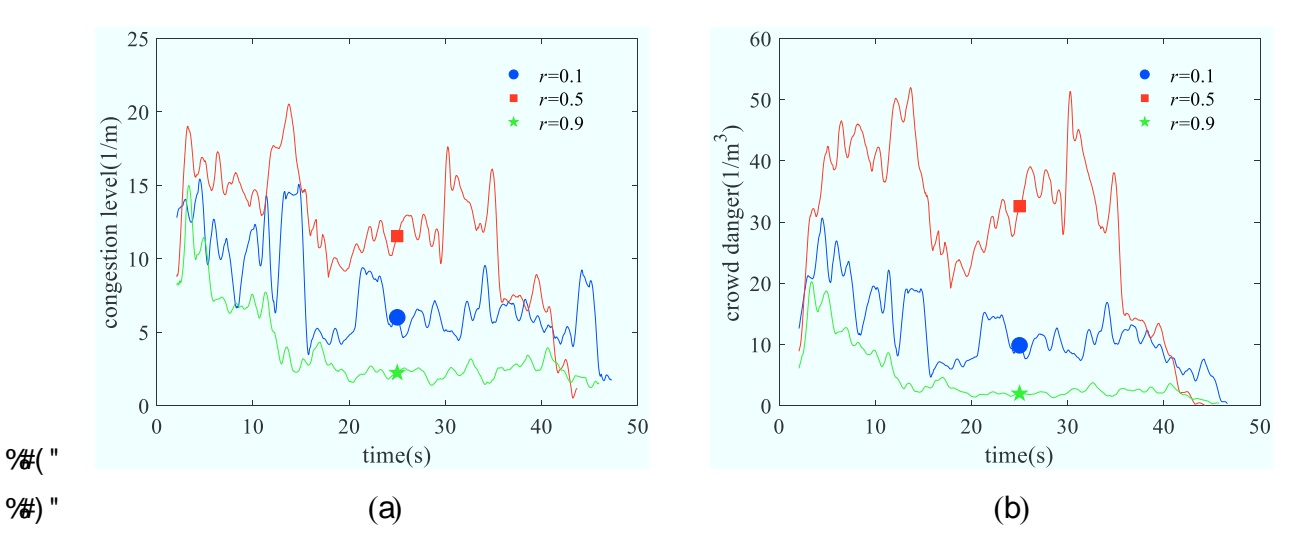


Figure 13. Time series data in three different runs with the flow ratio equal to 0.1, 0.5 and 0.9. (a) Congestion level. (b) Crowd danger.

%#* "

%+"

%! " %#"

%\$\$"

%%% %&"

% "

%\$("

%\$)"

%*"

%/+"

%%"

%#"

%\\$"

%%%

%&" %%"

%%"

%%)" %%"

%\+"

%! "

To further examine the effect of flow ratio on the rotation range, congestion level and crowd danger, we plot the data from different runs together in the same figures as shown in figure 14. Due to the large fluctuations in the time series data, for certain runs, all these three quantities show wide ranges in the boxes. However, similar to the plot of individual ttc, just by looking at the average or median values, we can find something that makes sense. With the increase of flow ratio, the average/median values will increase first and then decrease, with the peak approximately appearing at the flow ratio of 0.5, and such trend is more pronounced in the congestion level and crowd danger plots since the velocity magnitude and density are further considered, compared with the rotation range plot. The highest average/median values occurring at r=0.5 indicate that the balanced bidirectional flow on stairs is the most dangerous and risky one, and for stairs where the bidirectional motion cannot be avoided, it is suggested that the numbers of pedestrians from two directions should be controlled intentionally to prevent the very balanced situation from happening. Again, for the bidirectional stair motion, its most special feature that can be distinguished from the plane motion is the asymmetry between the descending and ascending flows, which results in the asymmetric shapes that appear repeatedly in the plots of horizontal crossing speed, individual time to collision and finally the rotation range, congestion level as well as crowd danger.

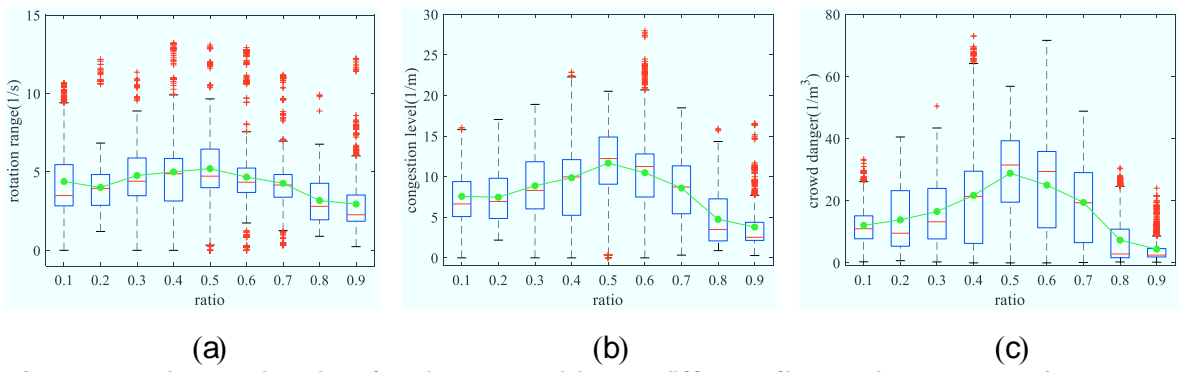


Figure 14. Time series data for three quantities at different flow ratios. (a) Rotation range. (b) Congestion level. (c) Crowd danger. The red '+' symbols represent the outliers.

Furthermore, we combine data from all nine runs to investigate the relations between density and congestion level as well as crowd danger. The results are shown in figure 15. Both the congestion level and crowd danger increase with density. Besides, similar to those in [30], these two relations can be fitted using the following equations:

$$\%(" \operatorname{Cd}(\rho) = \rho \cdot \operatorname{Cl}_{\text{max}}(1 - e^{-\kappa \rho}), \tag{10}$$

where Cl_{max} is the maximum value of congestion level and κ is a parameter used to represent the steepness of the fitting curve. According to the fitting results, Cl_{max} equals to 34.47 and κ equals to 0.1674. Although our data are a combination from uni- and bidirectional scenarios, we obtain similar value of κ with the bidirectional movement on the horizontal plane.

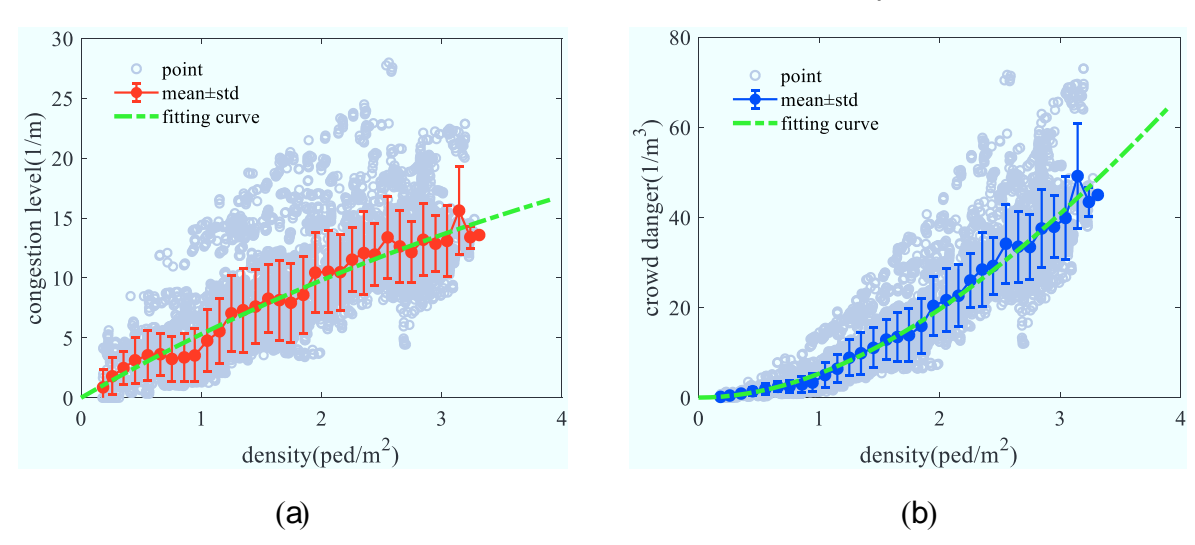


Figure 15. The relations between global density and global congestion level as well as crowd danger. (a) Congestion level. (b) Crowd danger. The solid circles and error bars represent the mean values and standard deviations, measured with a bin size of $0.1~\text{ped/m}^2$. The dash-dotted green curves are fitted based on the average values.

4. Conclusions and discussions

The stampede accident that happened in the New Year's Eve of 2015 in Shanghai due to the high density bidirectional pedestrian flow on stairs made us realize that how deficient is our knowledge about this kind of movement pattern. To get deeper insight into pedestrians' movement characteristics under such condition, we performed a controlled experiment on an outdoor staircase at varying flow ratios (from 0.1 to 0.9 with a step of 0.1) with up to 100 participants and analyzed the results based on the precise trajectories.

First of all, two measurements are employed to quantify pedestrians' crossing behaviors within the corridor, respectively the horizontal crossing speed and the offset distance. For both of the crossing speeds in the descending and ascending flows, a similar trend can be found that with the increase of flow ratio, they will decrease first and then increase. However, due to the effect of gravity, in average the ascending pedestrians are always slower than the descending ones. Besides, lateral movement is always larger than approximately $0.2 \, \text{m}$, reaching a considerably

! ("

,

%#"

%\$\$"

%%%

%&\"

%&)"

%*"

%+"

%!"

%#"

%\$"

%%

%&" %'"

%("

%)"

%*"

%+"

%!"

%#" %\$"

%% %&"

%'"

%("

%)"

%*"

%)+"

higher value when only 10% or 20% of pedestrians belong to the minor flow. Next, to obtain the fundamental diagrams that cover a wide range, the Voronoi-based method is applied to derive the density and velocity data. It is interesting to note that the average velocity, for each given density value, assumes always the lowest figure in the full bidirectional flow when compared with those in the descending and ascending flows, indicating that there exist much more complex interactions among pedestrians in the bidirectional situation. When comparing the bidirectional fundamental diagrams at varying flow ratios, the difference between the balanced and unbalanced runs is significant. On the other hand, the fundamental diagrams corresponding to well balanced flows (e.g., r=0.4, 0.5 and 0.6) have very similar flows, due to the comparable number of pedestrians in each flow. Furthermore, the time to collision is calculated and analyzed based on the smoothed trajectories. It's found that the average ttc can be used as a good indicator for the end of the full bidirectional state as the time when it begins to increase is almost consistent with that when the full bidirectional state ends. Also, our analysis about the relative positions for the paired pedestrians who are going to have the first collision implies that most first collisions happen in the same flow due to the stable lane formation in the experiment. Finally, judging from our analysis using rotation range, congestion level and crowd danger, the r=0.5 scenario appears to be the most dangerous and risky one, thus it is suggested that the very balanced situation should be avoided for stairs where bidirectional motion may occur. In conclusion, our results can be helpful for the calibration and validation of stair models and improving the design of stairs outdoors and in some transportation facilities.

Compared with the plane motion, the stair motion is more dangerous since pedestrians are easier to fall when walking on them. Most current studies about the stair motion are processed by using manual counting, thus exhibiting large discrepancies between literatures. In our future work, more trajectory-based analyses in complex building structures will be conducted, such as the merging process in the staircase with a large number of participants. Furthermore, due to the existence of steps, pedestrians' stepping behaviors may be different from those on the plane, it would be interesting to extract stepping parameters such as step length, step frequency, etc., from trajectories on stairs and make quantitative comparisons.

&+* " Acknowledgements

%!"

%#"

%\$"

%%

% &"

%)'"

%)("

%)"

%)*"

%+"

%!"

%#"

%\$"

%% %&"

%'"

%("

%)" %*"

&++"

&+! "

&+#"

&**+**\$"

&+%" &+&"

&+' "

&+("

&+)"

&! +" The authors acknowledge the foundation support from the National Key Research and &!!" Development Program (2018YFC0807000), National Natural Science Foundation of China &! #" (71804026, 71904006), Fundamental Research Funds for the Central &! \$" (WK2320000040). Mohcine Chraibi acknowledges the funding support from the Visiting Professor International project at the University of Science and Technology of China (Grant No. & % &! &" 2019A VR35). We want to thank Dr. Maik Boltes from the Juelich Supercomputing Center for &! ' " his help on extracting pedestrian trajectories on stairs. We also would like to thank Dr. Claudio &! (" Feliciani from the University of Tokyo for useful discussion about the congestion level.

&) " References

&! *" [1] R.F. Fahy, Overview of major studies on the evacuation of World Trade Center Buildings 1 8#+" and 2 on 9/11, Fire technology, 49 (2013) 643-655.

&#!" [2] J.D. Averill, D. Mileti, R. Peacock, E. Kuligowski, N. Groner, G. Proulx, P. Reneke, H. &##" Nelson, Federal Investigation of the Evacuation of the World Trade Center on September 11, &#\$" 2001, Fire & Materials, 36 (2012) 472-480.

- 8#% [3] E.R. Galea, L. Hulse, R. Day, A. Siddiqui, G. Sharp, The UK WTC 9/11 evacuation study: an
- &#&" overview of findings derived from first-hand interview data and computer modelling, Fire &
- 8#" Materials, 36 (2012) 501-521.
- 8#(" [4] R.D. Peacock, B.L. Hoskins, E.D. Kuligowski, Overall and local movement speeds during
- 8#) " fire drill evacuations in buildings up to 31 stories, Safety Science, 50 (2012) 1655-1664.
- 8#*" [5] F. Huo, W. Song, L. Chen, C. Liu, K. Liew, Experimental study on characteristics of
- &\$+" pedestrian evacuation on stairs in a high-rise building, Safety science, 86 (2016) 165-173.
- &\$! " [6] M. Delin, J. Norén, E. Ronchi, K. Kuklane, A. Halder, K. Fridolf, Ascending stair evacuation:
- &\$#" walking speed as a function of height, Fire and Materials, 41 (2017) 514-534.
- &\$\$" [7] J. Chen, J. Wang, B. Wang, R. Liu, Q. Wang, An experimental study of visibility effect on
- &\$% evacuation speed on stairs, Fire safety journal, 96 (2018) 189-202.
- &\$&" [8] Y. Zeng, W. Song, S. Jin, R. Ye, X. Liu, Experimental study on walking preference during
- &\$' " high-rise stair evacuation under different ground illuminations, Physica A: Statistical Mechanics
- **%**(" and its Applications, 479 (2017) 26-37.
- &\$) " [9] A.R. Larusdottir, A. Dederichs, Evacuation of children: movement on stairs and on horizontal
- **%***" plane, Fire technology, 48 (2012) 43-53.
- 8%" [10] Z.M. Fang, L.X. Jiang, X.L. Li, W. Qi, L.Z. Chen, Experimental study on the movement
- &%" characteristics of 5-6 years old Chinese children when egressing from a pre-school building,
- &/#" Safety science, 113 (2019) 264-275.
- &%" [11] E. Kuligowski, R. Peacock, E. Wiess, B. Hoskins, Stair evacuation of older adults and
- 8%% people with mobility impairments, Fire Safety Journal, 62 (2013) 230-237.
- 8% [12] E. Kuligowski, R. Peacock, E. Wiess, B. Hoskins, Stair evacuation of people with mobility
- &%" impairments, Fire and Materials, 39 (2015) 371-384.
- 8%" [13] F. Huo, W. Song, W. Lv, K.-M. Liew, Analyzing pedestrian merging flow on a floor-stair
- 8% " interface using an extended lattice gas model, Simulation, 90 (2014) 501-510.
- 8%" [14] G. Köster, D. Lehmberg, F. Dietrich, Is slowing down enough to model movement on
- **88+**" stairs?, in: Traffic and Granular Flow'15, Springer, 2016, pp. 35-42.
- &&! " [15] Y. Zeng, W. Song, F. Huo, G. Vizzari, Modeling evacuation dynamics on stairs by an
- 88#" extended optimal steps model, Simulation Modelling Practice and Theory, 84 (2018) 177-189.
- 88\$" [16] Y. Qu, Z. Gao, Y. Xiao, X. Li, Modeling the pedestrian's movement and simulating
- 88% evacuation dynamics on stairs, Safety science, 70 (2014) 189-201.
- 888" [17] M. Boltes, A. Seyfried, Collecting pedestrian trajectories, Neurocomputing, 100 (2013) 127-
- **&&**' " 133.
- 88(" [18] J. Chen, S. Lo, J. Ma, Pedestrian ascent and descent fundamental diagram on stairway,
- &&) " Journal of Statistical Mechanics: Theory and Experiment, 2017 (2017) 083403.
- &&* [19] S. Burghardt, A. Seyfried, W. Klingsch, Performance of stairs-fundamental diagram and
- &' +" topographical measurements, Transportation research part C: emerging technologies, 37 (2013)
- &'!" 268-278.
- & #" [20] L. Fu, S. Cao, Y. Shi, S. Chen, P. Yang, J. Fang, Walking behavior of pedestrian social
- &' \$" groups on stairs: a field study, Safety science, 117 (2019) 447-457.
- &' % [21] I. Cłapa, M. Cisek, P. Tofiło, M. Dziubiński, Firefighters ascending and evacuation speeds
- &' &" during counter flow on staircase, Safety science, 78 (2015) 35-40.
- &' " [22] S. Jiten, J. Gaurang, P. Purnima, A. Shriniwas, Effect of directional distribution on stairway
- & (" capacity at a suburban railway station, Transportation letters, 9 (2017) 70-80.
- &')" [23] X. Chen, J. Ye, N. Jian, Relationships and characteristics of pedestrian traffic flow in
- & * " confined passageways, Transportation Research Record, 2198 (2010) 32-40.

- & (+" [24] M. Liu, S. Wang, Y. Oeda, T. Sumi, Simulating uni-and bi-directional pedestrian movement
- &(!" on stairs by considering specifications of personal space, Accident Analysis & Prevention, 122
- **&**(#" (2019) 350-364.
- &(\$" [25] J. Zhang, W. Qiao, Y. Hu, S. Cao, X. Long, W. Song, The effect of a directional split flow
- &(% ratio on bidirectional pedestrian streams at signalized crosswalks, Journal of Statistical
- & (&" Mechanics Theory & Experiment, 2018 (2018) 073408-.
- &('" [26] B. Steffen, A. Seyfried, Methods for measuring pedestrian density, flow, speed and
- &((" direction with minimal scatter, Physica A Statistical Mechanics & Its Applications, 389 (2010)
- **&()** " 1902-1910.

&* **+**"

- &(*" [27] C. Feliciani, K. Nishinari, Empirical analysis of the lane formation process in bidirectional
- &) +" pedestrian flow, Phys.rev.e, 94 (2016) 032304.
- &)!" [28] I. Karamouzas, P. Heil, P.V. Beek, M.H. Overmars, A Predictive Collision Avoidance
- &) #" Model for Pedestrian Simulation, 2009.
- &) \$" [29] S. Holl, Methoden für die Bemessung der Leistungsfähigkeit multidirektional genutzter
- &) % Fußverkehrsanlagen, in, Universität Wuppertal, Fakultät für Architektur und
- &) &" Bauingenieurwesen ..., 2018.
- &)'" [30] C. Feliciani, K. Nishinari, Measurement of congestion and intrinsic risk in pedestrian
- &) (" crowds, Transportation Research Part C Emerging Technologies, 91 (2018) 124-155.
- &))" [31] D. Helbing, J. Anders, A.A. Habib Zein, Dynamics of crowd disasters: an empirical study,
- &) *" Physical Review E Statistical Nonlinear & Soft Matter Physics, 75 (2007) 046109.